

Primljen / Received: 9.12.2019.

Ispravljen / Corrected: 3.5.2020.

Prihvaćen / Accepted: 22.8.2020.

Dostupno online / Available online: 10.3.2021.

Extending service life of rails in the case of a rail head defect

Authors:



Assoc.Prof. **Dmitry Ovchinnikov**, PhD. CE
Samara state University of transport, Russia
Department of Railway and track facilities
sit@samgups.ru

Corresponding author



Prof. **Alexey Bondarenko**, PhD. CE
Samara state University of transport, Russia
Department of Railway and track facilities
bondarenko@infotrans-logistic.ru



Lei Kou, M.Sc. CE
TU Dresden, Germany
Institute of Railway Systems and Public Transport
kou.lei@tu-dresden.de



Assoc.Prof. **Mykola Sysyn**, PhD. CE
TU Dresden, Germany
Institute of Railway Systems and Public Transport
mykola.sysyn@tu-dresden.de

Research Paper

Dmitry Ovchinnikov, Alexey Bondarenko, Lei Kou, Mykola Sysyn

Extending service life of rails in the case of a rail head defect

Rails are subjected to the processes of wear, corrosion and contact and bending fatigue during their lifecycle. As a result of these processes, various types of damage and defects are formed in rails. The residual life of rails depends on the size, position, and orientation of defects. Maximum permissible crack-size values are calculated in this paper using the finite element method. The crack plane orientation relative to the contact surface plane is analysed. The dependence of the stress intensity factor on the crack area is established. This allows continued use of defective rails and safe operation on low-activity railways.

Key words:

railway track, rail defects, finite element method, crack

Prethodno priopćenje

Dmitry Ovchinnikov, Alexey Bondarenko, Lei Kou, Mykola Sysyn

Produljenje uporabljivosti tračnica u slučajevima oštećenja njihove glave

Tračnice su tijekom svoje uporabe izložene procesima trošenja, korozije i kontaktnog zamora uslijed savijanja. Kao posljedica tih procesa, na tračnicama dolazi do raznih oštećenja i neispravnosti. Nastavak uporabljivosti tračnica ovisi o veličini, položaju i smjeru oštećenja. U ovom su radu izračunane maksimalno dopuštene vrijednosti veličine pukotine metodom konačnih elemenata. Smjer ravnine pukotine analiziran je u odnosu na ravninu kontaktne površine kotač-tračnica. Utemeljena je ovisnost faktora veličine naprezanja o površini pukotine. To omogućuje daljnju upotrebu oštećenih tračnica i siguran nastavak rada na željezničkim prugama sa slabijom aktivnošću.

Ključne riječi:

željeznička pruga, oštećenja tračnice, metoda konačnih elemenata, pukotina

Vorherige Mitteilung

Dmitry Ovchinnikov, Alexey Bondarenko, Lei Kou, Mykola Sysyn

Verlängerung der Verwendbarkeit von Schienen bei Schäden des Schienenkopfes

Während ihrer Verwendung sind Schienen aufgrund von Biegung den Prozessen von Verschleiß, Korrosion und Kontaktermüdung ausgesetzt. Infolge dieser Prozesse treten verschiedene Schäden und Mängeln an den Schienen auf. Die weitere Verwendbarkeit der Schienen hängt von der Größe, Position und Richtung des Schadens ab. In dieser Arbeit werden die maximal zulässigen Werte der Rissgröße nach der Finite-Elemente-Methode berechnet. Die Richtung der Rissebene wurde in Bezug auf die Ebene der Rad-Schiene-Kontaktfläche analysiert. Die Abhängigkeit des Spannungsgrößenfaktors von der Rissoberfläche wurde bestimmt. Dies ermöglicht die weitere Verwendung beschädigter Schienen und die sichere Fortsetzung des Betriebs auf Eisenbahnschienen mit weniger Aktivität.

Schlüsselwörter:

Eisenbahnschiene, Schienenbeschädigung, Finite-Elemente-Methode, Riss

1. Introduction

Railway track is an important part of the infrastructure, and its technical condition provides for general safety of traffic. The state of railway components is determined by their carrying capacity. The track superstructure is subjected to very harsh conditions: trains passing, exposure to wind, rain, and temperature changes. However, it is important to maintain, under these conditions, a sufficient strength and stability and ensure economic durability. Being the main bearing element of the railway superstructure, rails have to:

- withstand long-term train wheel load without cracks or other damage
- transfer load from wheels to rail bases, and ensure its distribution over a sufficiently large surface
- direct/guide movement of the wheels of rail vehicles.

In the course of railway operation, rails are subjected to various processes such as rail wear, plastic flow, corrosion, and fatigue, including also the process of contact bending and corrosion fatigue. Due to these processes, various types of damage and defects are formed.

A rail defect is characterized by deviation of its geometric parameters or strength from established specifications, provided that the rail operates in accordance with specified operating conditions. Rail defects include: head checks, shelling, spalling, squats, cracks, rolling contact fatigue, various types of wear, plastic deformations in the form of flow of rail heads, corrosion, mechanical damage, etc., if their amplitude exceeds prescribed values. Rail failure is classified as a defect if it brings about the need to stop the train (for example, complete failure with rail damage) or to limit the speed of the train (partial failure, such as running surface defects in track head, etc.) [1].

A frequent rail head defect is a transverse fatigue crack in the form of light or dark spots, due to contact fatigue of metal so that the metal strength is insufficient to form internal or external longitudinal cracks, and leads to failure after a maximum allowable tonnage is exceeded [2, 3]. (Figure 1).

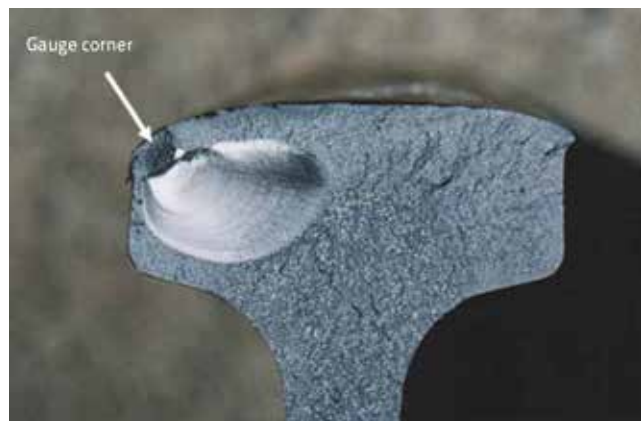


Figure 1. Representation of a rail head defect [8]

Defect occurs when an internal longitudinal crack, or longitudinal crack in the form of line along rail axis, forms from accumulation of non-metallic inclusions, elongated during rail rolling. The development of longitudinal cracks leads to formation of shelling or transverse cracks. When such cracks develop to a size exceeding the critical one (14 - 16 mm in height or 25-30% of the cross-sectional area of the head at temperatures above -20 ° C and from 15% at temperatures below -20 °C), transverse cracks can lead to the breaking of the entire rail [4]. A research on defect growth characterization in modern rail steels, as presented in paper [5], demonstrates high influence of rail heat treatment and nonuniform cooling on the microstructure and fatigue crack growth rate behaviour. Maintenance works like weld repairs are an additional source of rail fatigue, as such works increase the effect of residual stress on the crack growth rate as shown in [6].

The stress intensity factor (SIF) K , is used in fracture mechanics to predict the stress state near the tip of a crack or notch caused by an external load or residual stresses [7, 8]. The definition of K arose from the consideration of the problem of stresses in a body with a crack. The magnitude of K depends on sample geometry, the size and location of the crack, and the magnitude and distribution of loads on the material. It is assumed that arbitrary loading could be divided into three types of linearly independent cracking modes. These load types are considered as Modes I, II, and III. Mode I is a tensile mode in which crack surfaces directly separate from one another. Mode II is a plane shear mode in which crack surfaces slide over one another, perpendicular to the crack leading edge. Mode III is a tearing shear mode in which crack surfaces move relative to one another, parallel to the crack leading edge. The SIFs K_I , K_{II} and K_{III} correspond to the load cracking modes. These SIFs are formally defined as follows [9]:

$$\begin{aligned}
 K_I &= \lim_{r \rightarrow \infty} \sqrt{2\pi r} \sigma_{yy}(r, 0) \\
 K_{II} &= \lim_{r \rightarrow \infty} \sqrt{2\pi r} \sigma_{yx}(r, 0) \\
 K_{III} &= \lim_{r \rightarrow \infty} \sqrt{2\pi r} \sigma_{yz}(r, 0)
 \end{aligned}
 \tag{1}$$

where, σ_{ij} – distribution of stress components near the crack tip in polar coordinates r, θ with origin at the crack tip.

The stress field at the crack vertices has a singularity of the form $1/r^{0.5}$, where r is the distance from the crack vertex to the point where the stress is considered. The stress intensity factor is a measure of stress singularity in the vicinity of a crack. The dimension in the SI system is $\text{Pa}\cdot\text{m}^{0.5}$. It is suggested that the condition for the beginning of crack propagation can be formulated as the condition for stresses to reach critical values, thereby formulating a force criterion for brittle fracture.

The problem of the rolling contact fatigue initiation and development has been presented by many authors. These experimental investigations are presented in papers on the long term monitoring and analysis of crack development at

rail surface using a variety of technical means [10, 11]. The theoretical studies are usually based on the analytic Hertzian solution [12], semi-analytic FASTSIM algorithm [13, 14] and the finite element (FEM) simulations. The FEM simulation of stresses in the wheel rail interaction system is presented in studies [15-17]. An approach for determining a critical size for RCF (Rail Contact Fatigue) initiation from rail surface defects is presented in [18]. The methodology is based on the evaluation of stress of defects at the transient rolling contact, which takes into account the frictional rolling contact model. A prediction of RCF crack initiation life, with identification of crack plane orientation, is presented in [19]. The prediction is based on a dynamic three-dimensional FEM model and a simulation of axle box accelerations.

In this paper, mathematical models are developed for the limit state calculation and assessment of operational life of rails taking into account the head flange surface defects. The mathematical model allows determination of failure rate of the rail with head flange defects by describing the stress field at the crack tip. The following criteria are used for assessing critical K values [4, 20]:

- crack edges are displaced in the direction normal to the crack plane;
- crack edges are displaced in the plane of the crack normal to the crack propagation front;
- crack edges are displaced in the plane of the crack parallel to the crack propagation front.

2. Numerical FEM model for wheel and rail contact interaction

A volumetric finite element model FEM has been developed in the software ANSYS to analyse the stress intensity coefficient in the wheel and rail contact zone. The properties of the materials are completely identical to the properties of rail steel, and to the properties of wagon wheels. All elements are modelled with full geometric similarity to full-scale structures. The capacity of the static structural analysis model is about 400 thousand nodes of 75 thousand tetrahedral elements. The symmetry properties of the model are used to significantly reduce the number of finite elements. In the contact zone, the mesh of elements is noticeably detailed (element size is 0.5 mm) to enable the most accurate display of the analysis results. Such a small value of the element faces in the contact zone allows accurate simulation of the geometry of the real contact spot, as well as improvement of the accuracy of calculation results without significantly increasing the time spent on modelling (Figure 2.).

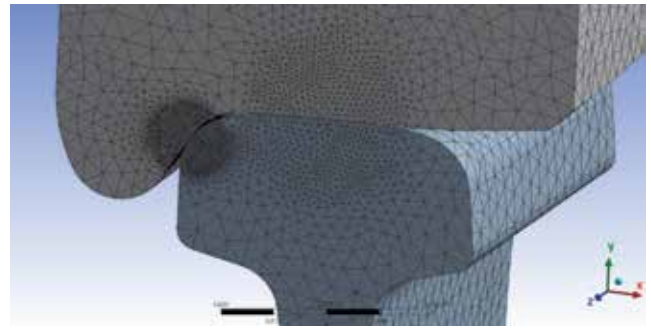


Figure 2. Finite element model for calculation at two-point contact

The following boundary conditions were used. Rigid contact is modelled along the area of the rail foot. The contact surface of the wheel and the axle moves with two - point contact-in the vertical and horizontal direction. Symmetric boundary conditions are also used. Other elements are not fixed. The simulation took into account lateral displacement of the wheel relative to the rail, which is considered as the distance between the axis of symmetry of the rail section and the plane of the wheel rolling circle. The transverse offset is zero if the wheel's rolling circle line is on the rail's axis of symmetry. The following parameters were used in the simulation: the rail profile R65 of rail steel R350HT according to the standard GOST R 51685-2013, the freight wagon wheel according to the standard GOST10791-2011 [21] with a diameter of 950 mm. Elastic properties of material are $E = 210\text{GPa}$ and $\nu = 0.3$. The axial load capacity amounts to 27 tons/axle, the lateral force is 10 tons, wheel axle is in vertical position, the rail inclination axis is 1/20, and the contact surfaces correspond to the specified profiles. The stress fields arising from this wheel-rail interaction are shown in Figure 3. As can be seen, the maximum stresses occur in the contact zone of the wheel and the lateral flange of the rail. It is obvious that the greatest SIF will be observed when the crack is located in the zone of maximum equivalent stresses (Figure 3).

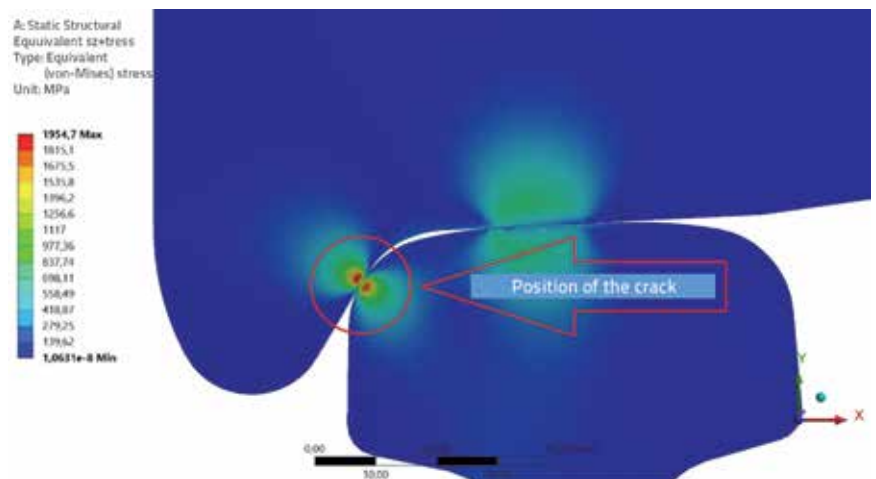


Figure 3. The stress distribution and location of the crack

3. Analysis of influence of crack size and orientation on stress intensity factor

Two cases of crack orientation are selected for the numerical simulation and analysis: the parallel and the perpendicular position to the rolling surface. Ten variants of crack size, with different values of length, width and thickness, are calculated for the two cases.

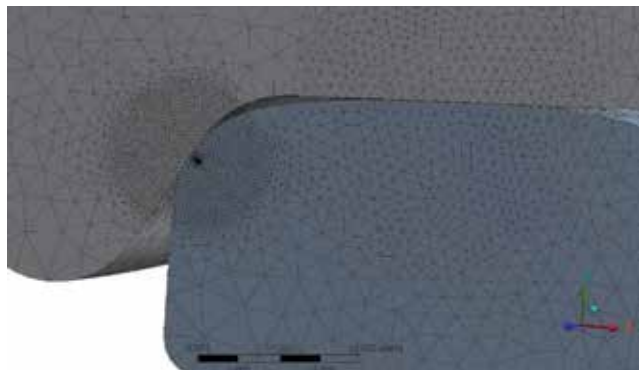


Figure 4. The FEM mesh for wheel and rail with a crack perpendicular to the wheel-rail contact

The model mesh for Case 1, in which the crack is perpendicular to the wheel and rail head contact, is shown in Figure 4. In the crack area, the grid becomes thicker and reaches the component size of 0.1 mm. The crack itself is elliptical in shape with a thickness of 0.01 mm in the rail.

The results of estimation of stress intensity coefficients at different geometrical parameters of elliptic crack are presented in Figures 5-ab. In the initial data studied, the maximum value of SIF is achieved when the load causes the edge of the crack to shift in the direction normal to the crack plane. The results of SIF calculation for all Case 1 variants are presented in Table 1.

An approximation of the dependence of the stress intensity coefficient on the crack area is presented in Figure 6. The figure shows the most intensive SIF development up to about 1 mm² in area. After that, the increase of the SIF is almost linearly proportional to the increase in crack area.

According to relevant standards [21], maximum permissible values of K for rails produced in various countries are shown in Table 2.

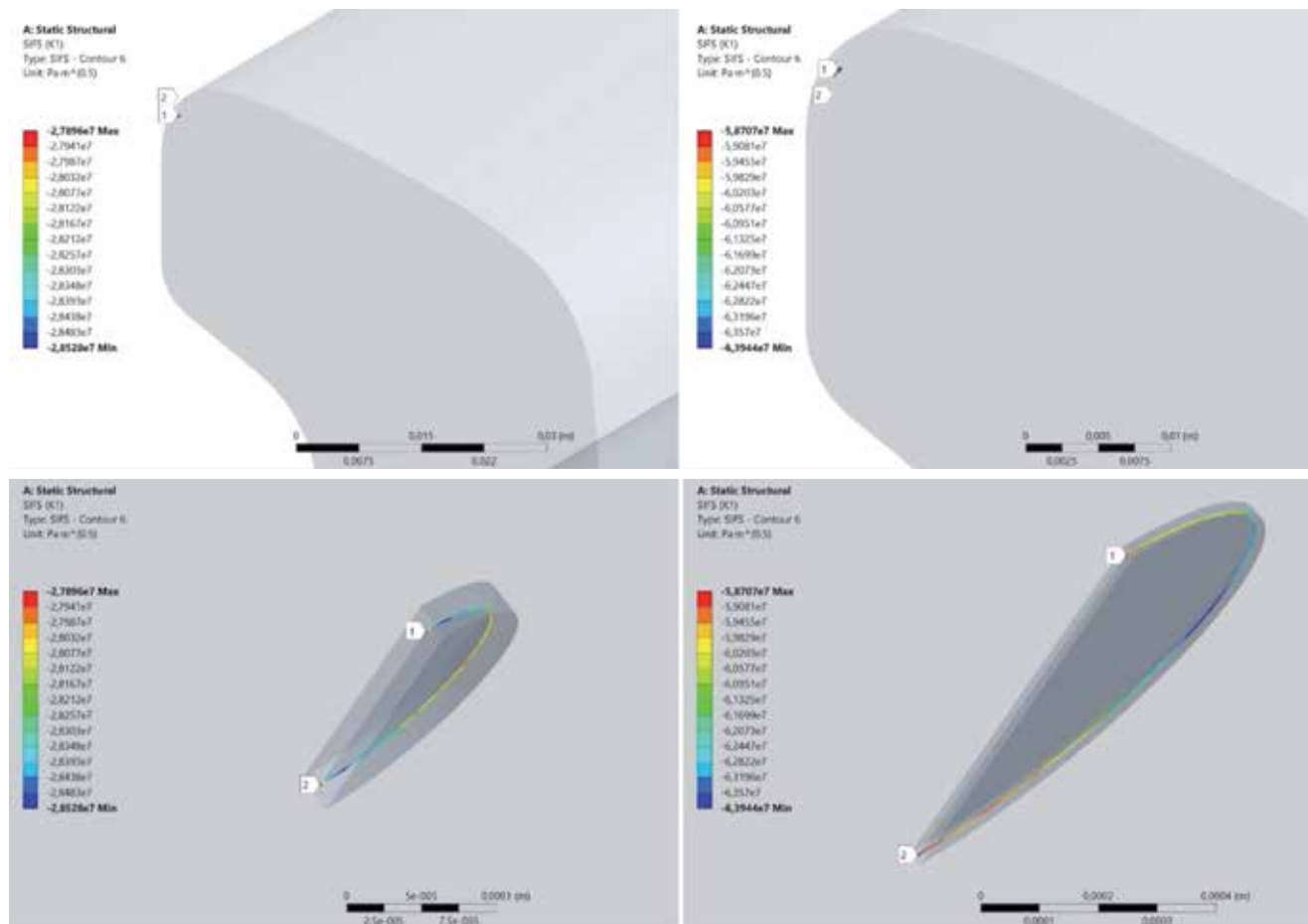


Figure 5. SIF of elliptical shape crack that is parallel to contact surface with axle sizes: 0.1 x 0.1 [mm] (left); 0.5 x 0.5 [mm] (right)

Table 1. Results of modelling crack SIF at two-point contact of wheel and rail for crack that is parallel to contact surface

Crack size [mm]			K_{III} [MPa·m ^{0.5}]			Area [mm ²]	The max value [MPa·m ^{0.5}]
Length	Width	Thickness	K_I	K_{II}	K_{III}		
0.1	0.1	0.01	28.5	2.7	3.5	0.032	28.5
0.1	0.25	0.01	38	3.1	2	0.078	38
0.25	0.25	0.01	44.1	5.9	2.8	0.196	44.1
0.25	0.5	0.01	56.7	6.7	2	0.392	56.7
0.5	0.25	0.01	58.2	9.3	6.4	0.392	58.2
0.5	0.5	0.01	64	12.1	5.4	0.786	64
0.5	1	0.01	80.5	14.6	3.9	1.57	80.5
1	0.5	0.01	83.4	20.7	14.1	1.57	83.4
1	1	0.01	94.1	26.9	12.2	3.142	94.1
2	1	0.01	123	27.8	25.7	6.284	123

Table 2. Rail steel fatigue limit of full-profile rails and cyclic crack resistance values after cyclic test results

Country of manufacture	Fatigue limit [MPa]	Crack resistance [MPa·m ^{0.5}]
Russia, NKMK (T1)	400	41-59
Russia, NTMK(T1)	407	46-56
France	477	-
Japan, NS	430	26-38
Canada	453	-
Austria	423	25-36
Italy	366	25-29
Poland	367	29-31

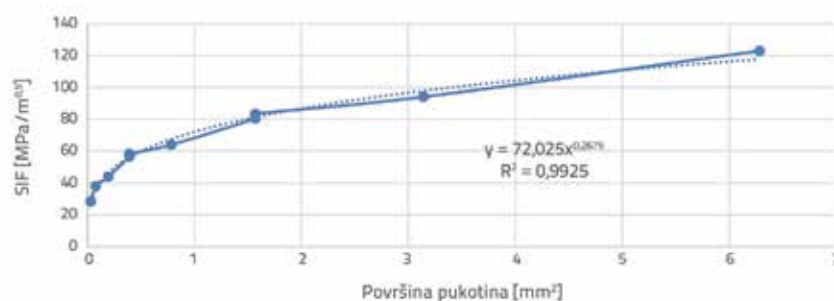


Figure 6. Dependence of stress intensity coefficient on crack area

Table 3. Results of modelling crack development at two-point contact of wheel and rail for crack that is perpendicular to contact surface

Crack size [mm]			K_{III} [MPa·m ^{0.5}]			Area [mm ²]	The max value [MPa·m ^{0.5}]
Length	Width	Thickness	K_I	K_{II}	K_{III}		
0.1	0.1	0.01	6.7	2	1.5	0.032	6.7
0.1	0.25	0.01	8.8	2.5	1.1	0.078	8.8
0.25	0.1	0.01	8.8	2.2	2.1	0.078	8.8
0.25	0.25	0.01	12.5	3.5	2.2	0.196	12.5
0.25	0.5	0.01	15.5	4.1	1.8	0.392	15.5
0.5	0.5	0.01	24.4	5.8	3.3	0.786	24.4
0.75	0.5	0.01	36.1	8.2	4.6	1.178	36.1
0.75	0.75	0.01	42.7	6.5	4.4	1.768	42.7
0.75	1	0.01	47	10	4	2.356	47

Thus, when the K value is close to the endurance limit of the rail, the amplitude of crack growth increases significantly, up to destruction of the rail. Based on mathematical modelling, the critical area of the crack - the maximum area of the beam - can be determined, after which the crack growth will be accelerated, leading to further destruction of the rail. For the elliptical crack perpendicular to the plane of contact between the wheel and rail, the maximum allowable value of this area is 0.2 mm². The influence of geometric parameters of the crack and its location relative to the reaction under contact of wheel and rail was evaluated in this paper. Figure 6 shows that the maximal admissible area of cracks can be increased by reducing the loading. This fact can be used for extending the service life of the rails, through their recycling, on the low-activity and smaller

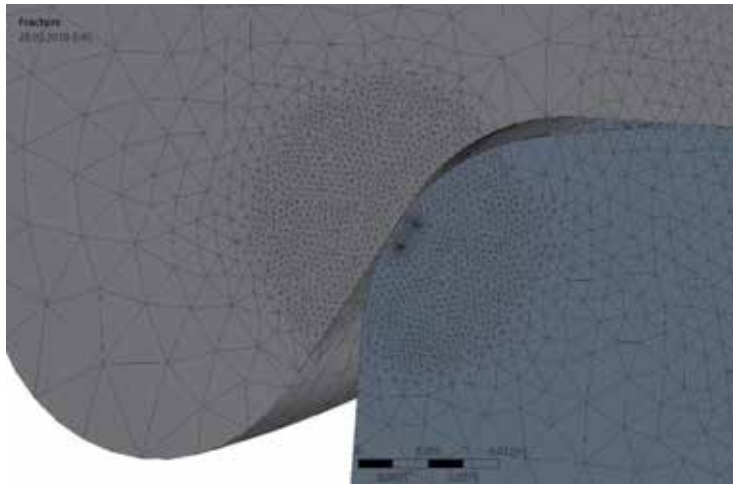


Figure 7. FE mesh in the presence of a crack parallel to normal wheel-rail interaction reaction

traffic-load railways. The model mesh for Case 2, in which the crack is parallel to the wheel and rail head contact, is shown in Figure 7. In the cracked area, the mesh is densified to a component size of 0.1 mm. The crack itself is a bundle of elliptical shapes with a track thickness of 0.01 mm.

The results of estimation of stress intensity coefficients at different geometrical parameters of elliptic crack are shown in Figure 8. The maximum value of SIF loading cracking modes occurs in the load situation in which the edges of the crack are shifted in the direction normal to the plane of the crack.

Unlike Case 1, a maximum crack size of 0.75 x 1.0 mm is selected. Calculation results for ten crack size variants are presented in Table 3.

The calculation results show that the critical SIF value reached is not possible when the crack is parallel to the wheel-rail contact plane, compared

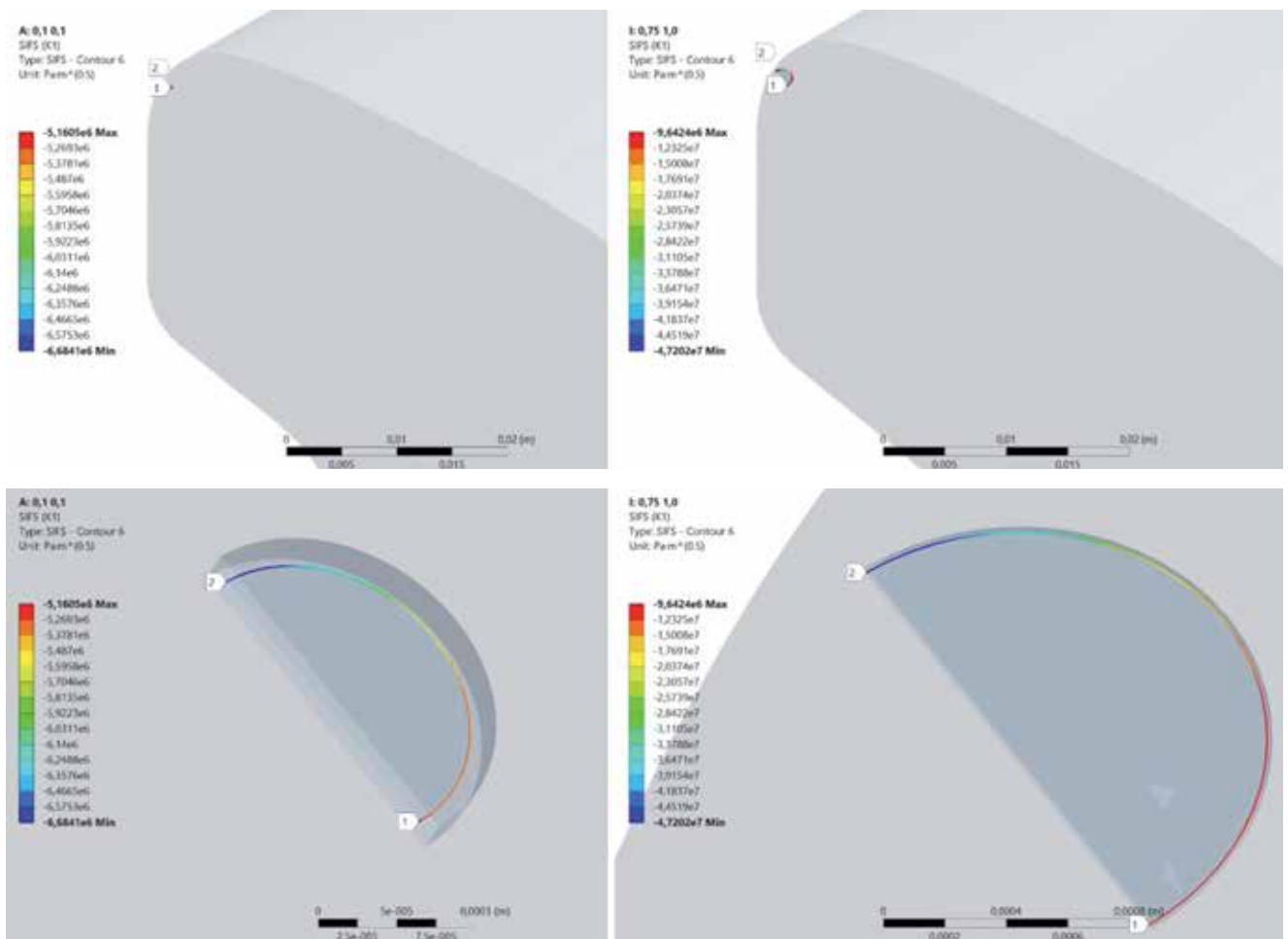


Figure 8. SIF of elliptically shaped crack that is perpendicular to contact surface with axle sizes: 0.1 x 0.1 [mm] (left); 0.75 x 1.0 [mm] (right)

to the crack perpendicular to the wheel-rail contact reaction plane. The maximum allowable crack area increases from 0.2 mm² to about 2 mm². Thus, the development of a crack parallel to the contact reaction plane is extremely unlikely.

4. Conclusion

The FEM simulation model of double contact interaction between the rail and wheel is developed. The model takes into account concentration of internal tensions due to cracks of different size and orientation. The stress field at the crack tip is estimated utilizing the stress intensity factor that is used

to measure the stress concentration point near the crack. The relationship between the stress intensity coefficient and the crack area is analysed: the maximum allowable crack area of the elliptical crack perpendicular to the wheel-rail contact reaction plane is 0.1 mm². The crack orientation parallel to the plane of the wheel-rail contact interaction is analysed. The results show that the cracks parallel to the contact reaction plane have much lower influence on SIF than perpendicular ones.

The service life of the rails with cracks can be significantly extended through their recycling and use on the low-activity and smaller traffic-load railways.

REFERENCES

- [1] Tselko, A.V.: The Defects in rails - classification, catalogue and parameters of defective and acute defective rails, October 23, 2014 No. 2499r, Vice-President of Russian Railways, Joint Stock Company "Russian Railways", Moscow, Russia.
- [2] UIC Code 712 Rail Defects, Fourth edition, International Union of Railways, pp. 111, 2002.
- [3] Rail Corp Engineering Manual Track: Rail Defects Handbook. ART Corporation, 2006
- [4] Abdurashitov, A., Yu., Ovchinnikov, D.V., Poccocki, V. A.: Development with application of methods of mathematical modeling of the profile of the tread surface of the wheel rim truck of the car adapted to the profile of the unworn surface of the rail R-65. Collection of works of scientists of JSC "VNIIZHT" (JSC "Scientific-research Institute of railway transport"), Moscow, pp. 30-59, 2017.
- [5] Jeong, D.Y., Woelke, P.B., Nied, H.F., DuPont, J.N., Kizildemir, S., Fletcher, F.B., Hutchinson, J.W.: Defect growth characterization in modern rail steels, Joint Rail Conference, Snowbird, Paper No.: JRC2019-1265, 2019.
- [6] Jun, H.K., Seo, J.W., Jeon, S., Lee, S.H., Chang, Y.S.: Fracture and fatigue crack growth analyses on a weld-repaired railway rail, Engineering Failure Analysis, 59 (2016), pp. 478-492, <https://doi.org/10.1016/j.engfailanal.2015.11.014>
- [7] Anderson, T.L.: Fracture mechanics: fundamentals and applications, Third edition, CRC Press, 2005.
- [8] Polevoi, E.V., Yunin, G.N., Smirnov, L.A.: Rail Quality Standards and Monitoring, Steel in Translation, 49 (2019) 7, pp. 496-498, <https://doi.org/10.3103/S096709121907009X>.
- [9] Suresh, S.: Fatigue of Materials. Cambridge University Press, (2004) ISBN 978-0-521-57046-6.
- [10] Zgutova, K., Neslusan, M., Sramek, J., Danisovic, P., Capek, J.: Monitoring of surface damage in rails after long term cyclic loading, Communications - Scientific Letters of the University of Zilina, 19 (2017) 2, pp. 153-158.
- [11] Sysyn, M., Gerber, U., Nabochenko, O., Gruen, D., Kluge, F.: Prediction of Rail Contact Fatigue on Crossings Using Image Processing and Machine Learning Methods, Urban Rail Transit, 5 (2019) 2, pp. 123-132, <https://doi.org/10.1007/s40864-019-10105-0>
- [12] Meymand, S.Z., Keylin, A., Ahmadian, M.: A survey of wheel-rail contact models for rail vehicles, Vehicle System Dynamics, 54 (2016) 3, pp. 386-428, <https://doi.org/10.1080/00423114.2015.1137956>
- [13] Spiriyagin, M., Polach, O., Cole, C.: Creep force modelling for rail traction vehicles based on the Fastsim algorithm. Vehicle System Dynamics, 51 (2013), pp. 1765-1783.
- [14] Vollebregt, E.A.H.: FASTSIM with Falling Friction and Friction Memory, Noise and Vibration Mitigation for Rail Transportation Systems, Volume 126 of the series "Notes on Numerical Fluid Mechanics and Multidisciplinary Design", pp. 425-432, 2015.
- [15] Milošević, M., Miltenović, A., Banić, M., Tomić, M.: Determination of residual stress in the rail wheel during quenching process by FEM simulation, Mechanical Engineering, 15 (2017) 3, pp. 413-425, <https://doi.org/10.22190/FUME170206029M>
- [16] El-sayed, H.M., Lotfy, M., Zohny, E.H.N., Riad, H.S.: Prediction of fatigue crack initiation life in railheads using finite element analysis, Ain Shams Engineering Journal, 9 (2018) 4, pp. 2329-2342, <https://doi.org/10.1016/j.asej.2017.06.003>
- [17] Muravev, V.V., Tapkov, K.A., Volkova, L.V., Platunov, A.V.: Strain stress model of the rail with crack in its head and estimation of its operational lifetime, Materials Science Forum, 970 (2019), pp. 177-186, <https://doi.org/10.4028/www.scientific.net/MSF.970.177>
- [18] Li, Z., Zhao, X., Dollevoet, R.: An approach to determine a critical size for rolling contact fatigue initiating from rail surface defects, International Journal of Rail Transportation, 5 (2017) 1, pp. 16-37, <https://doi.org/10.1080/23248378.2016.1194775>
- [19] Martua, L., Ng, A.K., Sun, G.: Prediction of Rail Rolling Contact Fatigue Crack Initiation Life via Three-Dimensional Finite Element Analysis, 8th International Conference on Intelligent Rail Transportation, London, 2018, <https://doi.org/10.1109/ICIRT.2018.8641633>
- [20] Romanowicz, P.: Numerical assessment of fatigue load capacity of cylindrical crane wheel using multiaxial high-cycle fatigue criteria, Archive of Applied Mechanics, 87 (2017) 10, pp. 1707-1726, <https://doi.org/10.1007/s00419-017-1281-6>
- [21] GOST 10791-2011, All-rolled wheels-specification, 2012. <http://www.gostrf.com/normadata/1/4293800/4293800552.pdf>